Differential effects of ketoconazole and primaquine on the pharmacokinetics and tissue distribution of imatinib in mice

Gian Wan Soo, Jason H.K. Law, Elaine Kan, Shin Yee Tan, Wei Yin Lim, Grace Chay, Nadeem I. Bukhari and Ignacio Segarra

Imatinib, a selective inhibitor of c-KIT and Bcr-Abl tyrosine kinases, approved for the treatment of chronic myelogenous leukemia and gastrointestinal stromal tumors, shows further therapeutic potential for gliomas, glioblastoma, renal cell carcinoma, autoimmune nephritis and other neoplasms. It is metabolized by CYP3A4, is highly bound to α-1-acid glycoprotein and is a P-glycoprotein substrate limiting its brain distribution. We assess imatinib's protein binding interaction with primaquine, which also binds to α-1-acid glycoprotein, and its metabolic interaction with ketoconazole, which is a CYP3A4 inhibitor, on its pharmacokinetics and biodistribution. Male ICR mice, 9–12 weeks old were given imatinib PO (50 mg/kg) alone or co-administered with primaquine (12.5 mg/kg), ketoconazole (50 mg/kg) or both, and imatinib concentration in the plasma, kidney, liver and brain was measured at prescheduled time points by HPLC. Noncompartmental pharmacokinetic parameters were estimated. Primaquine increased 1.6-fold plasma $AUC_{0\rightarrow\infty}$, C_{Max} decreased 24%, T_{Max} halved and $t_{1/2}$ and mean residence time were longer. Ketoconazole increased plasma $AUC_{0\rightarrow\infty}$ 64% and doubled the C_{Max}, but this dose did not affect $t_{1/2}$ or mean residence time. When ketoconazole and primaquine were co-administered, imatinib $AUC_{0\rightarrow\infty}$ and C_{Max} increased 32 and 35%, respectively. Ketoconazole did not change imatinib's distribution efficiency in the liver and kidney, primaquine increased it two-fold and it was larger when both the drugs were co-administered with imatinib. Ketoconazole did not change brain penetration but primaquine increased it approximately three-fold. Ketoconazole and primaquine affect imatinib clearance, bioavailability and distribution pattern, which could improve the treatment of renal and brain tumors, but also increase toxicity. This would warrant hepatic and renal functions monitoring. ***Anti-Cancer Drugs*** **21:695–703 © 2010 Wolters Kluwer Health | Lippincott Williams & Wilkins.**

Anti-Cancer Drugs 2010, **21**:695–703

Keywords: bioavailability, drug–drug interaction, imatinib, ketoconazole, primaquine, tissue distribution

Department of Pharmaceutical Technology, School of Pharmacy and Health Sciences, International Medical University, Kuala Lumpur, Malaysia

Correspondence to Dr Ignacio Segarra, PhD, Department of Pharmaceutical Technology, School of Pharmacy and Health Sciences, International Medical University, No. 126 Jalan 19/155 B, Bukit Jalil, 57000 Kuala Lumpur, Malaysia
Tel: +60 3 2731 7237; fax: +60 3 8656 7229;
e-mail: segarra100@gmail.com

Received 30 December 2009 **Revised form accepted** 28 May 2010

Introduction

Imatinib is a selective, rationally designed, c-KIT and Bcr-Abl tyrosine kinase inhibitor, approved for the treatment of chronic myelogenous leukemia (CML) [1], gastrointestinal stromal tumors (GIST) [2,3] and unresectable GIST [4]. Human and preclinical studies have suggested that imatinib may be beneficial in other diseases including glioma [5], rheumatic diseases [6], autoimmune nephritis [7] and renal cell carcinoma [8]. Mechanistically, imatinib blocks cell proliferation and induces apoptotic cell death in Bcr-Abl positive cells. Imatinib occupies the ATP-binding pocket and maintains the Bcr-Abl oncogenic fusion protein in an inactive form, which leads to growth inhibition of leukemic and clonogenic bone marrow cells in CML patients [9]. In addition, imatinib also inhibits the autophosphorylation of platelet-derived growth factor receptor and c-Kit tyrosine kinases [10]. Activated platelet-derived growth factor receptor drives the development of glioblastoma, a primary tumor of the central nervous system, whereas c-Kit is implicated in the development of GIST and small cell lung carcinoma [11].

Imatinib is a quadrivalent base (p*K*a = 1.52–8.07), freely soluble in water at a pH lower than 5.5 and stable in gastrointestinal fluid, which leads to high bioavailability (98%). In humans, the half-life is 13–18 h [12] and it is extensively metabolized mainly by CYP3A4 and CYP3A5, although CYP2D6 and CYP2C9 are minor contributors, into an active metabolite (CGP 74588) with a longer half-life (40 h) [12]. Both imatinib and the main metabolite are excreted in bile into the intestine where it may undergo enterohepatic recycling. It is mostly excreted through the feaces and only around 5% is excreted unchanged in urine [13].

Imatinib binds to α-1-acid glycoprotein, a single-chain glycoprotein (MW 36 000–44 000) synthesized in the liver that binds basic and neutral lipophilic drugs and its plasma concentration is 0.5–1.4 mg/ml in humans with a free fraction around 3.1% [14,15]. Imatinib's affinity to human α-1-acid glycoprotein is higher than to albumin with affinity constants of 4.9×10^6 and 2.3×10^5 l/mol, respectively, which has therapeutic implications. Clinical

0959-4973 © 2010 Wolters Kluwer Health | Lippincott Williams & Wilkins DOI: 10.1097/CAD.0b013e32833c93b3

trials have shown that there is no effect of albumin concentration on imatinib efficacy [16], unlike α-1-acid glycoprotein that has significant consequences. Leukocytic patients with elevated plasma α-1-acid glycoprotein levels had decreased free imatinib fraction and showed reduced efficacy [15]. Some CML and GIST patients showed only transient response and developed resistance despite a high plasma imatinib concentration. However, leukemic cells from these patients tested *in vitro* showed remission at the same concentration found in plasma. This suggests a limiting effect of imatinib α-1-acid glycoprotein binding on the free imatinib available *in vivo* [15]. In mice, increased imatinib tissue distribution was observed after co-administration with clindamycin [15], erythromycin [17] and metronidazole [18], suggesting a limiting role of efflux transporters, especially MRP1 and P-glycoprotein (P-gp) [19,20], together with a low partition coefficient ($\log P = 1.267$ at 37°C) [21] in its tissue penetration. Finally, although imatinib is well tolerated in general, it has also shown renal and hepatic toxicity including several fatal outcomes [22,23]. Severe hepatotoxicity was shown in patients [23] and in preclinical animal models alone or in combination with other drugs [24,25].

In this study, we assessed the changes in systemic and tissue exposure of imatinib caused by the inhibition of first-pass effect and protein displacement using two model drugs. First, we assess the effect of ketoconazole–imatinib interaction on the pharmacokinetics and tissue exposure of imatinib. Ketoconazole, an antifungal drug, commonly used by cancer patients is a potent CYP450 3A4 inhibitor able to affect imatinib's bioavailability [26]. Second, we evaluate the effect of protein-binding inhibition on tissue penetration using primaquine, an antimalarial drug, which, similar to imatinib, preferentially binds to the α-1-acid glycoprotein (affinity constant value of 4.0×10^5 l/mol) than human serum albumin (affinity constant value $\sim 0.6 \times 10^4$) [27]. Finally, the extent of imatinib penetration in the tissues of interest was evaluated after the co-administration of both ketoconazole and primaquine. Specifically, the brain and kidney were chosen because of imatinib's potential to treat glioblastoma [5] and renal cell carcinoma [8], and the liver was chosen because of severe hepatoxicity associated with imatinib [23].

Materials and methods

Reagents and drugs

Imatinib mesylate (Cipla Ltd., India), ketoconazole (Sigma-Aldrich, USA) and primaquine (Merck, Germany) were stored protected from light and refrigerated. HPLC grade methanol and acetonitrile were purchased from Merck (Germany). Triethlylamine (Nacalai Tesque Inc., Japan), glacial acetic acid (J.T. Baker, Thailand) were of analytical grade and sodium chloride (Promega, USA) of molecular grade. Ethanol 95% was supplied by HmbG Chemicals (Hamburg, Germany) and heparin sodium was purchased from Sigma-Aldrich (Germany).

Experimental animals and study design

Male ICR mice of similar age (8–12 weeks) and weight (18–25 g) were supplied by the Universiti Putra Malaysia (Kuala Lumpur, Malaysia), housed in the Animal Holding Facility of the International Medical University under a 12-h light cycle, provided with food and water *ad libitum* and allowed to acclimatize for at least 1 week prior before the procedure. All study procedures were approved by the Institutional Animal Use and Research Ethics Committee.

Before dosing, the mice were fasted for 12 h (water *ad libitum*) and randomly assigned to either the control or study groups. Mice in the control group were administered 50 mg/kg of imatinib orally with a 22G feeding needle (Braintree Scientific Inc., USA) attached to a 1 ml syringe (Terumo Corp., Philippines). Mice in the study group I were administered 50 mg/kg ketoconazole orally 15 min before the oral dose of imatinib (50 mg/kg) and mice in the study group II were administered primaquine 12.5 mg/kg orally 20 min before the oral dose of imatinib (50 mg/kg). Mice in the study group III were administered primaquine (12.5 mg/kg), followed by ketoconazole (50 mg/kg) 5 min later and imatinib (50 mg/kg) 15 min after ketoconazole administration. The dosing volume was adjusted such that the total would not exceed 0.4 ml. Four mice were used for each time point (2, 5, 10, 20, 40 min, 1, 2, 4, 6, and 10 h post imatinib administration). The mice were killed by cervical dislocation, and blood collected through cardiac puncture to minimize the remaining blood in the tissues and plasma separated by centrifugation (1500 rpm, 10 min, 4°C). The tissues of interest, brain, liver and kidneys were harvested and rinsed thoroughly with 0.9% saline solution. Plasma and tissues were kept at −35°C until HPLC analysis.

Sample processing and analysis

Imatinib concentration in the plasma and tissues was measured using a validated HPLC method [28]. Plasma was added to an equal volume of methanol, vortex mixed, centrifuged (15 000 rpm, 15 min, 4°C) and 120 µl of supernatant transferred to HPLC microvials for injection [29]. The tissue samples were allowed to thaw and weighed, and the extraction solvent was added (40% water, 30% methanol, 30% acetonitrile, pH 4.00) to reach a 4 ml/g dilution for the brain and 10 ml/g for the kidneys and liver. The tissue samples were homogenized at 35 000 rpm and 500 µl of slurry was transferred to an Eppendorf vial, sonicated for 1 min, centrifuged (15 000 rpm, 15 min, 4°C) and 300 µl of the supernatant transferred to a HPLC microvial for injection. A 100 µl aliquot of the supernatant was injected onto an Inertsil CN-3 column (150 × 4.6 mm, 5 µm particle size) and eluted at a 1 ml/min flow rate with a mixture of 1% triethylamine, 35% methanol and pH 4.8 water in an

Agilent 1200 Series HPLC system. Imatinib was eluted at 7.5 min and was detected at 268 nm [28]. Quantification of imatinib was carried out using an external calibration curve (linear range 0.1–25 μg/ml). Recovery from plasma and tissues was above 75%; intra-day and inter-day variability and accuracy was within 15%. The lower limit of quantification (LOQ) was 0.1 μg/ml, but imatinib could be detected at 0.05 μg/ml (data below the LOQ were treated as zero). The samples were free of matrix interference, and neither ketoconazole nor primaquine interfered with imatinib detection.

Pharmacokinetic analysis

Pharmacokinetic analysis was performed using noncompartmental techniques. The elimination rate constant (k_{el}) was calculated from the log-linear regression of the terminal slope of the concentration-time curve. The half-life ($t_{1/2}$) was calculated by $\ln 2/k_{el}$ and the area under the curve from time zero to the last concentration ($AUC_{0-t\ last}$) was calculated using the log-trapezoidal rule. The extrapolated AUC to infinity ($AUC_{t\ last\rightarrow\infty}$) was calculated as the last measured concentration divided by the elimination rate constant, C_{last}/k_{el}, and the total exposure ($AUC_{0-\infty}$) was the addition of the $AUC_{0\rightarrow t\ last}$ and the $AUC_{t\ last\rightarrow\infty}$. The maximum concentration (C_{Max}) and the time to C_{Max} (T_{Max}) were determined directly from the concentration–time graph of imatinib in the plasma and tissues. Apparent clearance (Cl/*F*) was calculated as $D/AUC_{0\rightarrow\infty}$, wherein D represents the dose. The mean residence time (MRT) was calculated as $AUMC_{0\rightarrow\infty}/AUC_{0\rightarrow\infty}$, wherein AUMC is the area under the first moment versus time curve from time zero to infinity. The apparent volume of distribution at steady state, V_{SS}/F was calculated as MRTxCl/*F*.

In some tissues, imatinib exposure was evaluated only up to the last measureable concentration ($AUC_{0-t\ last}$) because it was not possible to obtain a clear disposition constant. Changes in exposure were analyzed using the methodology proposed by Bailer for the comparison of AUC constructed with sparse sampling [30,31].

Results

Plasma pharmacokinetics of imatinib

Co-administration of ketoconazole, primaquine or both significantly affected the disposition profile of imatinib (Fig. 1, Table 1). Imatinib (control group) was rapidly absorbed and displayed a two-phase disposition profile with a fast decline followed by a slower elimination phase. This profile was consistent with a two-compartment model or a two-phase disposition profile found earlier in mice [29,32]. Co-administration with ketoconazole or primaquine caused a large increase of exposure. However, after co-administration with ketoconazole and primaquine together, the imatinib pharmacokinetic profile after the T_{Max} showed a rapid decline followed by a prolonged plateau up to 6 h, which culminated in a quick and sudden drop of the plasma concentrations (Fig. 1).

When imatinib was co-administered with ketoconazole or primaquine, the T_{Max} was reached earlier than in the control group (Table 1). However, the imatinib C_{Max} increased two-fold after co-administration with ketoconazole and remained unchanged after primaquine co-administration, but did not reach statistical significance. Ketoconazole and primaquine increased imatinib $AUC_{0\rightarrow t\ last}$ (58 and 24%, respectively; $P < 0.001$) and the total exposure $AUC_{0\rightarrow\infty}$ (64 and 59%, respectively; $P < 0.001$). When ketoconazole and primaquine were

Fig. 1

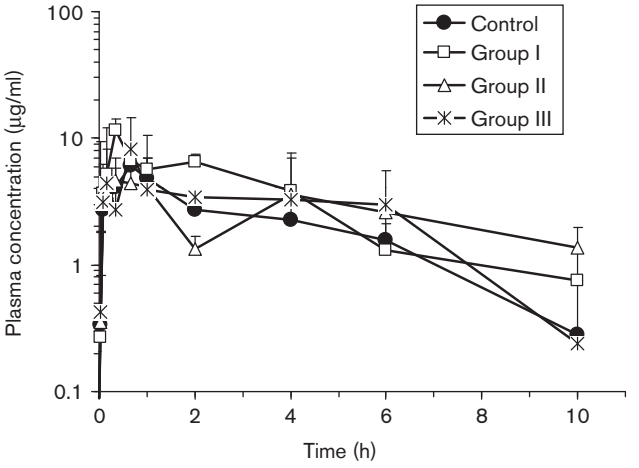

Pharmacokinetic profile of imatinib in the plasma after administration of 50 mg/kg (control) or co-administration of primaquine (12.5 mg/kg) or ketoconazole (50 mg/kg) or both the drugs to mice ($n=4$ per time point in each group).

Table 1 Model independent plasma pharmacokinetic parameters of imatinib in mice in control and study groups

Parameter	Control	Group I	Group II	Group III
Dose (mg/kg)				
Imatinib	50.0	50.0	50.0	50.0
Ketoconazole	–	50.0	–	50.0
Primaquine	–	–	12.5	12.5
C_{Max} (μg/ml)[a]	6.1 ± 1.9	11.6 ± 3.4	4.6 ± 0.9	8.3 ± 1.5
T_{Max} (min)	40	20	20	40
k_{el} (h)	0.293 ± 0.060	0.253 ± 0.099	0.160 ± 0.001	0.461 ± 0.144
$t_{1/2}$ (h)	2.4	2.7	4.3	1.5
$AUC_{0\rightarrow t\ last}$ (μg h/ml)[b]	20.7 ± 0.7	32.7 ± 1.6**	25.7 ± 1.2**	27.8 ± 1.3**
$AUC_{0\rightarrow\infty}$ (μg h/ml)[c]	21.5 ± 1.9	35.4 ± 4.1**	34.2 ± 4.3**	28.3 ± 3.0*
V_{SS}/F (l/kg)	8.10	5.25	10.60	6.56
Cl/*F* (l/h/kg)	2.31	1.40	1.46	1.77
MRT (h)	3.6	3.8	7.3	3.7

MRT, mean residence time.
[a]Mean ± SD.
[b]Mean ± SE, based on the Bailer's method for destructive sampling [30].
[c]Mean ± SD, based on the Yuan's extension to infinity of the Bailer's method [31].
*$P<0.01$.
**$P<0.001$.

co-administered together, the effects in plasma were less pronounced. Imatinib C_{Max} increased 35%, $AUC_{0\rightarrow\infty}$ increased 32% ($P < 0.001$) and there was no effect on T_{Max} (40 min). Co-administration reduced the oral clearance (Cl/*F*) 39, 37 and 24% in the study groups I, II and III, respectively. However, a change in pattern was observed on the apparent volume of distribution, (V_{SS}/F) which was lower than the control group in the study groups I and III (35 and 19%, respectively) but greater in group II. Finally, the MRT was similar in the study groups I and III and showed a two-fold increase after primaquine co-administration (group II).

Tissue distribution of imatinib in the control group

Imatinib showed good tissue penetration and distribution with concentrations higher in the tissue than in plasma, except for the brain with most of the concentrations below the LOQ, although imatinib could be detected in most of the samples. The kidneys and liver exhibited similar pharmacokinetic profiles (Fig. 2a). Before T_{Max} there was a fast drug uptake to reach C_{Max}, which was followed by a slow decline, almost plateau-like, leading to a faster disposition phase. Imatinib C_{Max} in the liver and kidneys was reached earlier and was higher than that in plasma, although only the liver C_{Max} showed statistical difference ($P < 0.001$). The largest tissue exposure was achieved in the kidney with three-fold greater $AUC_{0\rightarrow\infty}$ than the plasma followed by the liver (2.3-fold). In addition, the kidney tissue also presented the largest MRT (6.1 h). Imatinib did not penetrate the brain, and the brain C_{Max} was only *22%* than the C_{Max} found in the plasma ($P < 0.05$). The total imatinib brain exposure was minimal in the control group (Table 2).

Effect of drug interaction on the tissue distribution of imatinib

Co-administration of a second drug with imatinib changed the tissue distribution (Fig. 2) and the

Fig. 2

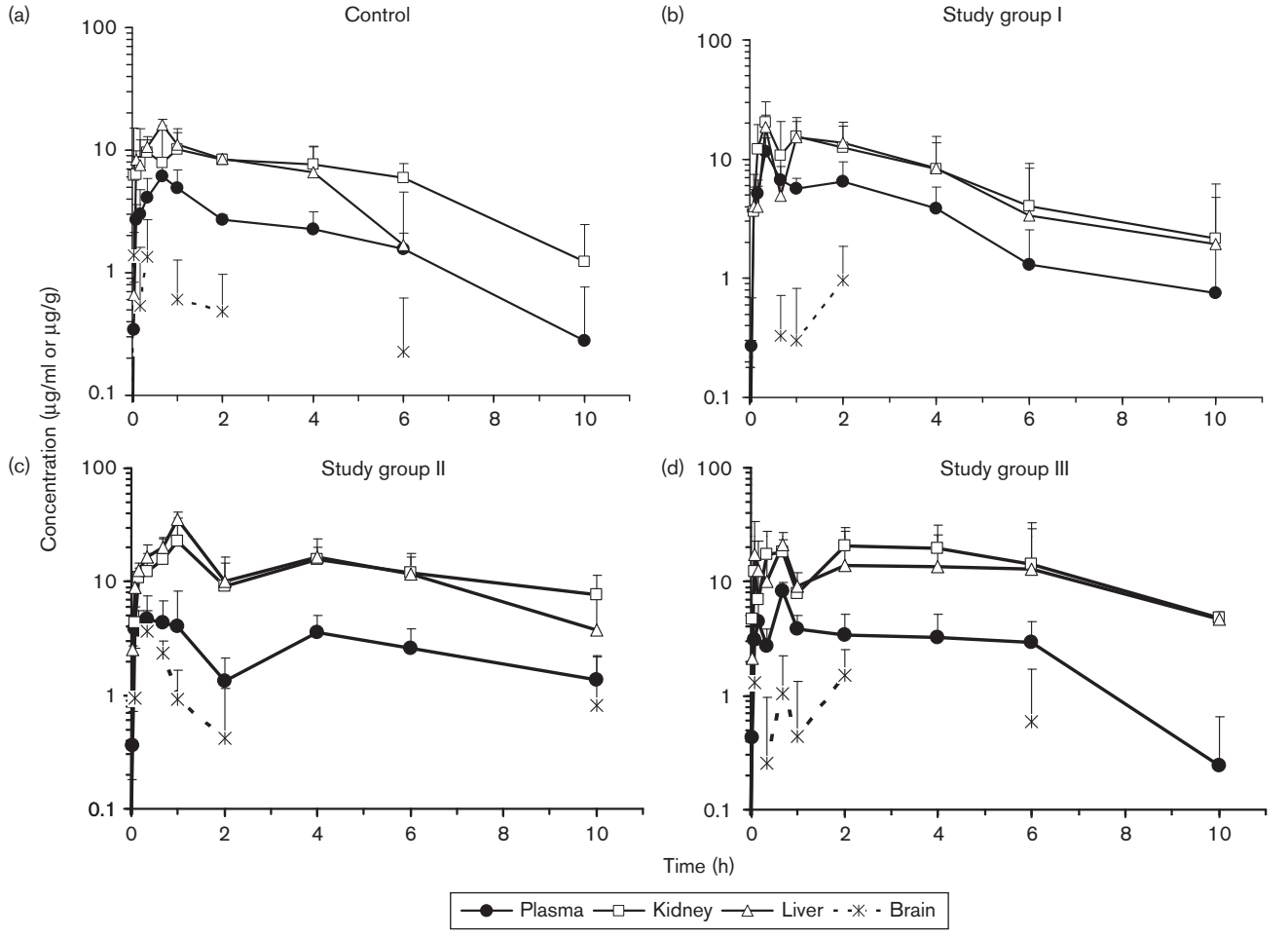

Pharmacokinetic profile of imatinib in the tissues after administration of 50 mg/kg oral imatinib (a) alone, (b) co-administration with 50 mg/kg oral ketoconazole, (c) co-administration with 12.5 mg/kg oral primaquine and (d) co-administration with primaquine (12.5 mg/kg) and ketoconazole (50 mg/kg), both orally. Concentration units are µg/ml (plasma) or µg/g (tissues) ($n = 4$ per time point in each group).

Table 2 Model independent pharmacokinetic parameters of imatinib in target tissues

Group	Tissue	C_{Max} (μg/g)	T_{Max} (min)	k_{el} (h^{-1})	$t_{1/2}$ (h)	$AUC_{0\rightarrow t\ last}$ (μg h/g)	$AUC_{0\rightarrow\infty}$ (μg h/g)	MRT (h)
Control	Liver	16.0 ± 1.7	40	0.355 ± 0.093	2.0	44.5 ± 2.5	49.2 ± 6.9	2.9
	Kidney	10.1 ± 4.5	60	0.317 ± 0.070	2.2	61.5 ± 2.4	65.5 ± 5.8	6.1
	Brain	1.3 ± 1.3	20	–	–	0.7 ± 0.1	–	–
Group I	Liver	18.4 ± 4.8	20	0.251 ± 0.044	2.8	68.8 ± 5.3**	75.7 ± 14.0**	4.3
	Kidney	20.5 ± 9.9	20	0.216 ± 0.049	3.2	72.6 ± 4.1**	82.5 ± 10.8**	4.6
	Brain	1.0 ± 0.9	120	–	–	0.9 ± 0.2	–	–
Group II	Liver	35.4 ± 13.2	60	0.251 ± 0.029	2.8	127.8 ± 5.1**	142.9 ± 15.2**	5.0
	Kidney	18.2 ± 11.5	60	0.117 ± 0.004	5.9	121.9 ± 3.0**	187.7 ± 8.8**	7.0
	Brain	3.7 ± 3.8	20	–	–	2.5 ± 0.2*	–	–
Group III	Liver	21.1 ± 5.8	40	0.141 ± 0.047	4.9	115.0 ± 9.9**	147.9 ± 28.2**	7.1
	Kidney	20.4 ± 9.2	120	0.189 ± 0.040	3.7	139.9 ± 9.1**	165.7 ± 22.6**	5.9
	Brain	1.5 ± 1.0	120	–	–	2.1 ± 0.5	–	–

MRT, mean residence time.
*$P<0.01$.
**$P<0.001$ in reference to control.

pharmacokinetics (Table 2). Ketoconazole, a CYP3A4 inhibitor and P-gp substrate [33], shortened the T_{Max} in the kidney and liver. The liver C_{Max} was slightly increased and the kidney C_{Max} increased two-fold, which was proportional to the plasma increase, although it was not statistically significant. In the liver, the elution rate constant decreased, the $t_{1/2}$ was slightly longer and the $AUC_{0\rightarrow\infty}$ was 1.5-fold greater ($P < 0.001$) than in the control group. Similarly, the kidney elution rate constant also decreased leading to a longer $t_{1/2}$ and 26% higher imatinib $AUC_{0\rightarrow\infty}$.

The effect of protein binding displacement on imatinib tissue distribution was assessed using primaquine that binds to α-1-acid glycoprotein [27]. Imatinib liver and kidney $AUC_{0\rightarrow\infty}$ after primaquine co-administration was 3.0 and 2.9-fold higher than in the control group, respectively. In addition, the liver and kidney C_{Max} were found to be 2.2 and 1.8-fold higher than in the control tissues, although they did not reach statistical significant differences ($P > 0.05$). The liver and kidney C_{Max} were 7.6 and 3.9-fold greater than the plasma C_{Max} ($P < 0.05$; $P < 0.001$ respectively). Tissue elution half-lives were slightly longer, but kidney MRT was shorter. Imatinib had better brain penetration after co-administration with primaquine as shown by a 2.7-fold increase in the C_{Max} and a 3.5-fold increase in the brain $AUC_{0\rightarrow t\ last}$ ($P < 0.01$). The pharmacokinetic profiles are shown in Fig. 2c and the pharmacokinetic parameters in Table 2.

Imatinib kidneys and liver concentrations were notably higher after co-administration with ketoconazole and primaquine together (Fig. 2d). Also evident in the pharmacokinetic disposition profile was the plateau-like shape up to 6 h. In the liver and kidney, T_{Max} was 40 and 120 min, respectively and C_{Max} was 31 and 100% higher, respectively. The total imatinib AUC was 3-fold greater than the control for the liver and 2.5-fold for the kidney. Finally, imatinib brain C_{Max} was slightly higher and a three-fold $AUC_{0\rightarrow last}$ increase was attained in this study group (Table 2).

Discussion

Drug–drug interactions in plasma

Ketoconazole and primaquine affected the pharmacokinetics of imatinib leading to a second peak and larger $AUC_{0\rightarrow\infty}$. Ketoconazole and primaquine administered together caused a plateau-like profile and greater exposure. Double-peak plasma concentration–time profiles have been observed for structurally diverse drugs and may be explained by the redistribution from the tissues and enterohepatic recycling [34], intestinal absorption windows [35], variable gastric emptying [36], physiological stress [37] or interaction between the drugs, bile salts and vehicle [38]. The double-peak phenomenon has not been observed for imatinib [29,32], but it may undergo enterohepatic recycling leading to the possibility of a second peak [13].

Ketoconazole, an inhibitor of CYP3A4, responsible for imatinib's metabolism [13], increased plasma C_{Max} and $AUC_{0\rightarrow\infty}$ 90 and 65%, respectively. The higher exposure may be attributed to first-pass metabolism inhibition rather than decreased systemic clearance, as changes in k_{el}, $t_{1/2}$ or MRT were not observed (Table 1). Ketoconazole's effect on first-past metabolism is also supported by the parallel decrease of oral clearance, Cl/F (−34%), and the apparent volume of distribution, V_{SS}/F (−40%), suggesting increased bioavailability only. These effects have been shown in patients taking imatinib and ketoconazole, wherein $AUC_{0\rightarrow\infty}$ increased 40% without changes in k_{el} or $t_{1/2}$ [26]. Ketoconazole shortened T_{Max} (20 min) suggesting faster absorption, possibly because of the inhibition of P-gp in the intestinal lumen [20]. These findings draw a parallel with studies showing that the low bioavailability in mice (27–37%) is mainly because of first-pass metabolism [32]. Primaquine co-administration increased $AUC_{0\rightarrow\infty}$ ($P < 0.001$). Primaquine inhibits CYP1A2 [39] and is a substrate of CYP3A4, CYP2E1, CYP2B6 and CYP2D6 [40,41], which are involved in imatinib biotransformation and may lead to higher exposure. Imatinib T_{Max} was shorter, probably also because of the inhibition of intestinal wall efflux pumps

[42,43]. Primaquine doubled the MRT suggesting that imatinib's displacement from α-1-acid glycoprotein and a higher plasma-free fraction leads to greater biodistribution and longer residence time in the system (Table 2).

Ketoconazole and primaquine have opposing effects on imatinib Cl/*F* and V_{SS}/F (Table 1). Study groups I and II showed 65% increased plasma $AUC_{0\rightarrow\infty}$ and −46% decreased Cl/*F*. However, the pattern changes for V_{SS}/F ketoconazole decreased V_{SS}/F 64.8% because of greater F, but primaquine caused a 31% increased of V_{SS}/F probably because of higher V_{SS} caused by protein displacement. Thus, the elimination $t_{1/2}$, related to Cl and the volume of distribution ($Cl = k_{el} \times V_d$) increased from 2.4 to 4.3 h.

Effect of ketoconazole and primaquine in tissue distribution

Primaquine and ketoconazole's first-pass inhibition increased plasma $AUC_{0\rightarrow\infty}$. Ketoconazole did not change the liver-to-plasma $AUC_{0\rightarrow\infty}$ ratio (2.3 ± 0.5 and 2.1 ± 0.6 for the control and group I, respectively) and only slightly reduced it in the kidney from 3.0 ± 0.5 to 2.3 ± 0.6 (Fig. 3). This suggests proportionality between tissue and plasma exposure (Table 2). In the liver, first-pass metabolism inhibition will increase plasma exposure, which is followed by proportional changes in liver exposure. On the other hand, the slight reduction of the kidney ratio may be associated with ketoconazole's vasoconstrictor effect [44,45], which may reduce the renal blood flow and the uptake capacity. Overall, ketoconazole does not seem to affect imatinib tissue uptake.

Liver and kidney exposure increased in a nonproportional manner in relation to plasma exposure after primaquine co-administration (Fig. 3). The tissue-to-plasma $AUC_{0\rightarrow\infty}$ ratio increased from 3.0 ± 0.5 to 5.5 ± 1.0 and from 2.3 ± 0.5 to 4.2 ± 1.0 in the kidney and liver, respectively (only the kidney ratio was significant, $P < 0.05$). This suggests that primaquine increased imatinib plasma exposure, displaced imatinib from the α-1-acid glycoprotein and increase tissue exposure and the volume of distribution (Table 2). When primaquine and ketoconazole were both administered together (group III), the tissue-to-plasma ratio was higher for the liver (5.2 ± 1.6) and kidney (5.9 ± 1.4) with *P* value of less than 0.05. This higher tissue penetration may show primaquine and ketoconazole's additive contributions to the inhibition of first-pass metabolism [39,43] and P-gp-mediated bile secretion [42].

Imatinib's brain exposure was minimal (Fig. 2). Although the brain is a highly perfused organ, the blood–brain barrier prevents the uptake of xenobiotics [46] and limits brain drug delivery [47]. Drug brain penetration correlates directly with lipophilicity and the uptake carriers' affinity but correlates inversely with the degree of ionization and protein binding [48]. Imatinib has a low partition coefficient; it is a substrate of several efflux transporters, which is highly bound to plasma proteins

Fig. 3

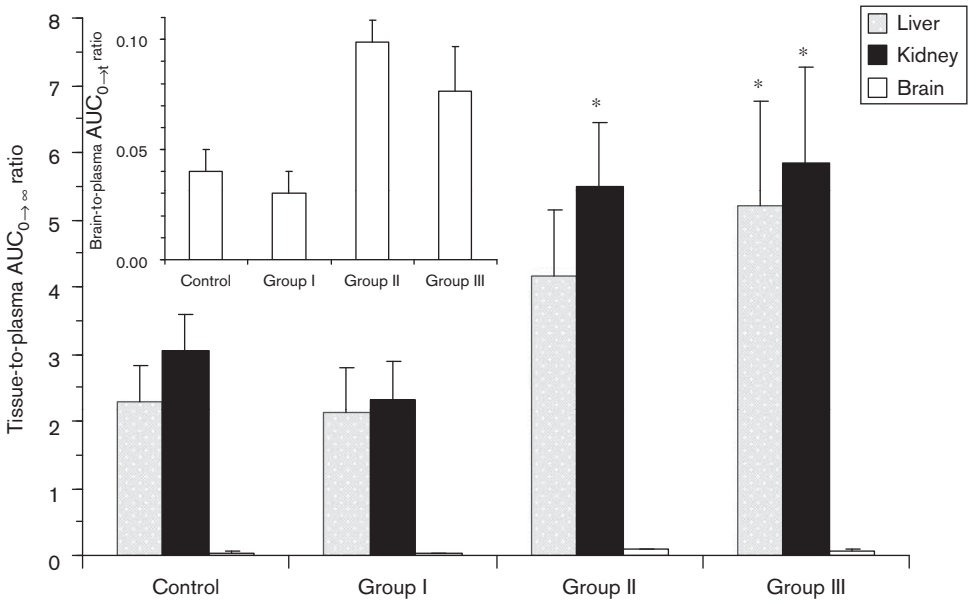

Efficacy of imatinib tissue penetration represented as the tissue-to-plasma $AUC_{0\rightarrow\infty}$ ratio for each study arm. The insert shows the ratio for the brain, which was calculated using $AUC_{0\rightarrow t}$ because of the absence of a clear terminal slope ($n = 4$ per time point in each group). *$P < 0.05$.

and is partially ionized at physiological pH [12]. These characteristics would explain its poor brain penetration. Ketoconazole's failure to increase imatinib brain exposure suggests that other transporters present at the blood–brain barrier, such as the breast cancer resistance protein, MRP1 [49] and hOCT1 [50] amongst others [47], would efflux imatinib masking ketoconazole's inhibition of P-gp. Finally, it cannot be excluded that the ketoconazole dose may inhibit the first-pass metabolism but may not be high enough to affect the blood–brain barrier. Higher brain uptake was observed after primaquine co-administration ($P < 0.001$). The brain-to-plasma AUC_{0-last} ratio increased from 0.04 ± 0.01 (control group) to 0.10 ± 0.10 in group II and to 0.08 ± 0.02 in group III (Fig. 3, insert).

Effects on clearance and bioavailability

The changes in imatinib's plasma-free fraction (f_u) affect the volume of distribution and clearance, and have clinical consequences [15]. A higher amount of imatinib is distributed to the tissues and is eliminated. Imatinib is mostly eliminated through P450 metabolism and presents a moderate-to-high hepatic extraction ratio after oral administration to mice [32]. These disposition features and the changes in free fraction have shown to affect the pharmacokinetics and pharmacological activity in leukocytic patients [15].

The relationship between Cl, k_{el}, V_d and f_u shows changes in Cl because of the changes in f_u, denoted by the SG-study group, in equation 1 [32]:

$$\frac{Cl_{SG}}{Cl_{Control}} = \frac{k_{el\,SG}}{k_{el\,Control}} \times \frac{f_{u\,SG}}{f_{u\,Control}} \quad (1)$$

Assuming that the changes in tissue exposure are mostly related to the changes in the plasma-free fraction, then the changes in the tissue-to-plasma ratio in the presence and absence of a second drug would reflect the change in free fraction:

$$\frac{f_{u\,SG}}{f_{u\,Control}} = \frac{AUC^{SG}_{Tissue}/AUC^{SG}_{Plasma}}{AUC^{Control}_{Tissue}/AUC^{Control}_{Plasma}} \quad (2)$$

Equation 2 estimates the free-fraction changes occurring in a second condition (e.g. drug co-administration, change in the route of administration, etc); and equation 1 relates them to clearance. Calculation of bioavailability assumes constant clearance and although this is probably a 'best guess' postulation, if protein binding is affected it may not be accurate. Bioavailability changes may be estimated as follows:

$$\frac{F_{SG}}{F_{Control}} = \frac{Cl_{SG}}{Cl_{Control}} \times \frac{AUC^{SG}_{Plasma}}{AUC^{Control}_{Plasma}} \quad (3)$$

in which $Cl_{SG}/Cl_{control}$ can be calculated using equations 1 and 2, assuming equal doses. These equations have limitations, e.g. the uptake mechanism should be concentration dependent or linear in nature; but may provide insights of the changes taking place.

Using the liver and kidney tissue-to-plasma ratios in the control and the study groups, the relative change in f_u (equation 2), Cl (equation 1) and bioavailability (equation 3) were estimated [32]. After the co-administration of ketoconazole (group I), the clearance was 0.72-fold lower and the bioavailability was 1.18-fold greater than in the control group. In group II, the clearance remained unchanged (relative change was 0.99), but bioavailability was 58% higher than in the control group (1.58-fold). In group III, a more extensive effect was noted: Cl and bioavailability were 3.3 and 4.3-fold higher than in the control group, respectively.

The findings suggest that metabolism and protein binding drug–drug interactions have effects beyond those observed in the plasma profile [18]. In the study group III, AUC increased 32% but the underlying pharmacokinetic change shows a 3.3-fold higher clearance equivalent to a 4.3-fold exposure increase. Conversely, ketoconazole caused a 64% increase in AUC, but it was only an 18% increase in bioavailability together with a 28% decrease in clearance. Thus, plasma AUC changes fall short to reflect the full extent of the interaction. Data to characterize the metabolite kinetics using mass spectrometry and further elucidate the mechanism of the interaction were not available, as it was beyond the analytical capacity of our laboratory.

Clinical implications

Imatinib has shown severe hepatic [23] and renal toxicity [22]. Generally, toxicity reversal is possible on imatinib discontinuation or dose reduction [51]. Drug interactions with imatinib may have also contributed to fatal outcomes [23]. In mice, paracetamol, commonly used for cancer pain management, caused changes in imatinib bioavailability [29] and increased hepatotoxicity including necrosis [24,25]. However, higher tissue exposure may allow further clinical applications. Philadelphia (Ph +) leukemia patients could overcome resistance mediated by high levels of α-1-acid glycoprotein [52]; higher kidney exposure may improve renal cell carcinomas treatments. Imatinib may be a new option to treat gliomas and glioblastoma, which until now has failed because poor brain biodistribution.

Conclusion

This study showed the potential impact that drug–drug interactions in protein binding and metabolism may have on imatinib disposition and tissue penetration. Although this study evaluates the extent of the drug–drug interactions in mice, translatability of the principles underlying these interactions to clinical scenarios may lead to ensure better pharmacological activity. In addition,

because of the α-1-acid glycoprotein concentration variability and its critical role in imatinib pharmacokinetics, it is suggested to monitor the plasma concentration of the α-1-acid glycoprotein during imatinib treatment. This, in turn, may lead to the optimization of therapeutic regimes and the success of treatment in cancer patients.

However, the potential for greater toxicity associated with higher imatinib concentrations in tissues should also be taken into account. Thus, methods to detect early signs of toxicity, e.g. monitoring liver and kidney function biomarkers, may be recommended.

Acknowledgement

The authors thank the International Medical University for the research grant B01/05-Res(05)2008.

References

1 Deininger M, Buchdunger E, Druker BJ. The development of imatinib as a therapeutic agent for chronic myeloid leukaemia. *Blood* 2005; **105**:2640–2653.
2 Dagher R, Cohen M, Williams G, Rothmann M, Gobburru J, Robbie G, *et al.* Approval summary: imatinib mesylate in the treatment of metastatic and/or unresectable malignant gastrointestinal stromal tumours. *Clin Can Res* 2002; **8**:3034–3038.
3 Kingham TP, Dematteo RP. Multidisciplinary treatment of gastrointestinal stromal tumors. *Surg Clin North Am* 2009; **89**:217–233.
4 Demetri GD, Wang Y, Wehrle E, Racine A, Nikolova Z, Blanke CD, *et al.* Imatinib plasma levels are correlated with clinical benefit in patients with unresectable/metastatic gastrointestinal stromal tumors. *J clin Oncol* 2009; **27**:3141–3147.
5 Wen PY, Yung AWK, Lamborn KR, Dahia PL, Wang Y, Peng B, *et al.* Phase I/II Study of imatinib mesylate for recurrent malignant gliomas. *Clin Cancer Res* 2006; **12**:4899–4907.
6 Paniagua RT, Robinson WH. Imatinib for the treatment of rheumatic diseases. *Nat Clin Pract Rheumatol* 2007; **3**:190–191.
7 Sadanaga A, Nakashima H, Masutani K, Miyake K, Shimizu S, Igawa T, *et al.* Amelioration of autoimmune nephritis by imatinib in MRL/lpr mice. *Arthritis Rheum* 2005; **52**:3987–3996.
8 Li G, Gentil-Perret A, Lambert C, Genin C, Tostain J. S100A1 and KIT gene expressions in common subtypes of renal tumour. *Eur J Surg Oncol* 2005; **31**:299–303.
9 Peng B, Hayes M, Resta D, Racine-Poon A, Druker BJ, Talpaz M, *et al.* Pharmacokinetics and pharmacodynamics of imatinib in a phase I trial with chronic myeloid leukemia patients. *J Clin Oncol* 2004; **22**:935–942.
10 Buchdunger E, Cioffi CL, Law N, Stover D, Ohno-Jones S, Druker B, Lydon NB. Abl protein-tyrosine kinase inhibitor STI571 inhibits in vitro signal transduction mediated by c-Kit and platelet-derived growth factor receptors. *J Pharmacol Exp Ther* 2000; **295**:139–145.
11 Krystal GW, Honsawek S, Litz J, Buchdunger E. The selective kinase inhibitor STI571 inhibits small cell lung cancer growth. *Clin Cancer Res* 2000; **6**:3319–3326.
12 Peng B, Lloyd P, Schran H. Clinical pharmacokinetics of imatinib. *Clin Pharmacokinet* 2005; **44**:879–894.
13 Gschwind HP, Pfaar U, Waldmeier F, Zollinger M, Sayer C, Zbinden P, *et al.* Metabolism and disposition of imatinib in healthy volunteers. *Drug Metab Dispos* 2005; **33**:1503–1512.
14 Fournier T, Medjoubi NN, Porquet D. Alpha-1-acid glycoprotein. *Prot Struc Mol Enz* 2000; **1482**:157–171.
15 Gambacorti-Passerini C, Zucchetti M, Russo D, Frapolli R, Verga M, Bungaro S, *et al.* Alpha-1-acid glycoprotein binds to imatinib (STI571) and substantially alters its pharmacokinetics in chronic myeloid leukemia patients. *Clin Cancer Res* 2003; **9**:625–632.
16 Judson I, Peiming M, Peng B, Verweij J, di Paola ED, van Glabbeke M, *et al.* Imatinib pharmacokinetics in patients with gatrointestinal stromal tumor: a retrospective population pharmacokinetic study over time. *Cancer Chemother Pharmacol* 2005; **55**:379–386.
17 Azuma M, Nishioka Y, Aono Y, Inayama M, Makino H, Kishi J, *et al.* Role of alpha 1-acid glycoprotein in therapeutic antifibrotic effects of imatinib with macrolides in mice. *Am J Respi Crit Care Med* 2007; **176**:1243–1250.
18 Tan SY, Soo GW, Chay G, Law JHK, Lim WY, Kan E, *et al.* Metronidazole affects the tissue distribution of imatinib but does not change its plasma pharmacokinetics in mice. *Drug Met Rev* 2009; **41** (**Suppl**):37–38.
19 Muenster U, Grieshop B, Ickenroth K, Gnoth MJ. Characterization of substrates and inhibitors for the in vivo assessment of Bcrp mediated drug-drug interaction. *Pharm Res* 2008; **25**:2320–2326.
20 Bihorel S, Camenisch G, Lemaire M, Scherrmann JM. Influence of breast cancer resistance protein (Abcg2) and p-glycoprotein (Abcb1a) on the transport of imatinib mesylate (Gleevec) across the mouse blood–brain barrier. *J Neurochem* 2007; **102**:1749–1757.
21 Velpandian T, Mathur R, Agarwal NK, Arora B, Kumar L, Gupta SK. Development and validation of a simple liquid chromatography method with ultraviolet detection for the determination of imatinib in biological samples. *J Chromatogr B* 2004; **804**:431–434.
22 Foringer JR, Verani RR, Tjia VM, Finkel KW, Samuels JA, Guntupalli JS. Acute renal failure secondary to imatinib mesylate treatment in prostate cancer. *Ann Pharmacother* 2005; **39**:2136–2138.
23 Cross TJ, Bagot C, Portmann B, Wendon J, Gillett D. Imatinib mesylate as a cause of acute liver failure. *Am J Hematol* 2006; **81**:189–192.
24 Nassar I, Pasupati T, Segarra I, Judson JP. A histopathological study of increased hepatotoxicity after coadministration of imatinib and acetaminophen in a preclinical mouse model. *Hepatol Int* 2009; **3**:198–199.
25 Nassar I, Pasupati T, Judson JP, Segarra I. Histopathological study of the hepatic and renal toxicity associated with the coadministration of imatinib and acetaminophen in a preclinical mouse model. *Mal J Pathol* 2010; **32**:1–11.
26 Dutreix C, Peng B, Mehring G, Hayes M, Capdeville R, Pokorny R, Seiberling M. Pharmacokinetic interaction between ketoconazole and imatinib mesylate (Glivec) in healthy subjects. *Cancer Chemother Pharmacol* 2004; **54**:290–294.
27 Zsila F, Visy J, Mady G, Fitos I. Selective plasma protein binding of antimalarial drugs to α-1-acid glycoprotein. *Bioorg Med Chem* 2008; **16**:3759–3772.
28 Teoh M, Narayanan P, Moo KS, Radhakrishnan S, Pillappan R, Bukhari NI, Segarra I. HPLC determination of imatinib in plasma and tissues after multiple oral dose administration to mice. *Pak J Pharm Sci* 2010; **23**:35–41.
29 Nassar I, Pasupati T, Judson JP, Segarra I. Reduced exposure of imatinib after coadministration with acetaminophen to mice. *Indian J Pharmacol* 2009; **41**:167–172.
30 Bailer AJ. Testing for the equality of area under the curves when using destructive measurement techniques. *J Pharmacokinet Biopharm* 1988; **16**:303–309.
31 Yuan J. Estimation of variance for AUC in animal studies. *J Pharm Sci* 1993; **82**:761–763.
32 Teoh M, Radhakrishnan S, Moo KS, Narayanan P, Bukhari NI, Segarra I. Pharmacokinetics, tissue distribution and bioavailability of imatinib in mice after administration of a single oral and an intravenous bolus dose. *Lat Am J Pharm* 2010; **29**:428–435.
33 Kageyama M, Namiki H, Fukushima H, Ito Y, Shibata N, Takada K. In vivo effects of cyclosporin A and ketoconazole on the pharmacokinetics of representative substrates for P-glycoprotein and cytochrome P450 (CYP) 3A in rats. *Biol Pharm Bull* 2005; **28**:316–322.
34 Weitschies W, Bernsdorf A, Giessmann T, Zschiesche M, Modess C, Hartmann V, *et al.* The talinolol double-peak phenomenon is likely cased by presystemic processing after uptake from gut lumen. *Pharm Res* 2005; **22**:728–734.
35 Plusquellec Y, Campistron G, Staveris S, Barre J, Jung L, Tillement JP, Houin G. A double-peak phenomenon in the pharmacokinetics of veralipride after oral administration: a double-site model for drug absorption. *J Pharmacokin Biopharmaceut* 1987; **15**:225–239.
36 Wang Y, Roy A, Sun L, Lau CE. A double-peak phenomenon in the pharmacokinetics of alprazolam after oral administration. *Drug Met Dispos* 1999; **27**:855–859.
37 Gué M, Peeters T, Depoortere I, Vantrappen G, Buéno L. Stress-induced changes in gastric emptying, postprandial motility, and plasma gut hormone levels in dogs. *Gastroenterol* 1989; **97**:1101–1107.
38 Zhou H. Pharmacokinetic strategies in deciphering atypical drug absorption profiles. *J Clin Pharmacol* 2003; **43**:211–227.
39 Bapiro TE, Egnell AC, Hasler JA, Masimirembwa CM. Application of higher throughput screening (HTS) inhibition assays to evaluate the interaction of antiparasitic drugs with cytochrome P450s. *Drug Metab Dispos* 2001; **29**:30–35.

40 Ganesan S, Tekwani BL, Sahu R, Tripathi LM, Walker LA. Cytochrome P(450)-dependent toxic effects of primaquine on human erythrocytes. *Toxicol Appl Pharmacol* 2009; **241**:14–22.
41 Masimirembwa CM, Hasler JA, Johansson I. Inhibitory effects of antiparasitic drugs on cytochrome P450 2D6. *Eur J Clin Pharmacol* 1995; **48**:35–38.
42 Vezmar M, Georges E. Reversal of MRP-mediated doxorubicin resistance with quinoline-based drugs. *Biochem Pharmacol* 2000; **59**:1245–1252.
43 Cuong BT, Binh VQ, Dai B, Duw DN, Lovell CM, Rieckmann KH, Edstein MD. Does gender, food, or grapefruit juice alter the pharmacokinetics of primaquine in healthy subjects? *Br J Clin Pharmacol* 2006; **61**:682–689.
44 Ogden KK, Falck JR, Watts SW. The cytochrome p450 inhibitor ketoconazole potentiates 5-hydroxytryptamine-induced contraction in rat aorta. *J Pharmacol Exp Ther* 2007; **323**:606–613.
45 Proctor KG, Shatkin S, Kaminski PM, Falck JR, Capdevila JH. Modulation of arteriolar blood flow by inhibitors of arachidonic acid oxidation after thermal injury: possible role for a novel class of vasodilator metabolites. *Circulation* 1988; **77**:1185–1196.
46 Breedveld P, Pluim D, Cipriani G, Wielinga P, van Tellingen O, Schinkel AH, Schellens JH. The effect of Bcrp1 (Abcg2) on the in vivo pharmacokinetics and brain penetration of imatinib mesylate (Gleevec): implications for the use of breast cancer resistance protein and p-glycoprotein inhibitors to enable the brain penetration of imatinib in patients. *Cancer Res* 2005; **65**:2577–2582.
47 Roberts LM, Black DS, Raman C, Woodford K, Zhou M, Haggerty JE, *et al.* Subcellular localization of transporters along the rat blood–brain barrier and blood–cerebral–spinal fluid barrier by in vivo biotinylation. *Neuroscience* 2008; **155**:423–438.
48 Matheny CJ, Lamb MW, Brouwer KLR, Pollack GM. P-glycoprotein modulation. *Pharmacother* 2001; **21**:778–796.
49 Zhou L, Schmidt K, Nelson FR, Zelesky V, Troutman MD, Feng B. The effect of breast cancer resistance protein and P-glycoprotein on the brain penetration of flavopiridol, imatinib mesylate (Gleevec), prazosin, and 2-methoxy-3-(4-(2-(5-methyl-2-phenyloxazol-4-yl)ethoxy)phenyl)propanoic acid (PF–407288) in mice. *Drug Metab Dispos* 2009; **37**:946–955.
50 Thomas J, Wang L, Clark RE, Pimohamed M. Active transport of imatinib into and out of cells: implications for drug resistance. *Blood* 2004; **104**:3739–3745.
51 Ferrero D, Pogliani EM, Rege-Cambrin G, Fava C, Mattioli G, Dellacasa C, *et al.* Corticosteriods can reverse severe imantinb-induced hepatotoxicity. *Haematologica* 2006; **91**:e78–e80.
52 Shen T, Kuang YH, Ashby CR, Lei Y, Chen A, Zhou Y, *et al.* Imatinib and nilotinib reverse multidrug resistance in cancer cells by inhibiting the efflux activity of the MRP7 (ABCC10). *PLoS One* 2009; **4**:e7520.